

Cardiac SPECT Radiomics Features Repeatability and Reproducibility: A Multi Scanner Phantom Study

Mohammad Edalat-Javid¹, Isaac Shiri², Ghasem Hajianfar³, Hamid Abdollahi⁴, Niki Oveisi⁵, Mohammad Javadian⁶, Mojtaba Shamsaei Zafarghandi¹, Hadi Malek⁷, Ahmad Bitarafan-Rajabi^{7,8,9}, Mehrdad Oveisi^{2,10}

1. Faculty of Nuclear Engineering and Physics, Amirkabir University of Technology, Tehran, Iran
2. Division of Nuclear Medicine and Molecular Imaging, Department of Medical Imaging, Geneva University Hospital, CH-1211 Geneva 4, Switzerland
3. Rajaie Cardiovascular Medical and Research Center, Iran University of Medical Science, Tehran, Iran
4. Department of Radiologic Sciences and Medical Physics, Faculty of Allied Medicine, Kerman University, Kerman, Iran
5. School of Population and Public Health, The University of British Columbia, BC, V6T 1Z4, Canada.
6. Department of Computer Science, Kermanshah University of Technology, Kermanshah, Iran
7. Department of Nuclear Medicine and Molecular Imaging, Rajaie Cardiovascular, Medical, and Research Center, Iran University of Medical Sciences, Tehran, Iran
8. Cardiovascular Intervention Research Center, Rajaie Cardiovascular Medical and Research Center, Iran University of Medical Sciences, Tehran, Iran
9. Echocardiography Research Center, Rajaie Cardiovascular Medical and Research Center, Iran University of Medical Sciences, Tehran, Iran
10. Department of Computer Science, University of British Columbia, Vancouver BC, Canada

Corresponding Author: Isaac Shiri

Division of Nuclear Medicine and Molecular Imaging,
Department of Medical Imaging, Geneva University Hospital,
CH-1211 Geneva 4, Switzerland
Email: Isaac.sh92@gmail.com

Abstract

Background: The aim of this study was to assess the robustness of cardiac SPECT radiomics features against changes in imaging settings including acquisition and reconstruction settings.

Methods: Four scanners were used to acquire SPECT scans of a cardiac phantom with 5mCi of ^{99m}Tc . The effects of different image acquisition and reconstruction settings including the Number of View, View Matrix Size, attenuation correction, image reconstruction algorithm, number of iterations, number of subsets, type of filter, full width at half maximum (FWHM) of Gaussian filter, Butterworth filter order, and Butterworth filter cut-off were studied. In total 5263 different images were reconstructed. Eighty-seven radiomic features including first, second, and high order textures were extracted from images. To assess reproducibility and repeatability the coefficient of variation (COV) was used for each image feature over the different imaging settings.

Result: IDMN and IDN features from GLCM, RP from GLRLM, ZE from GLSZM, and DE from GLDM feature sets were the only features that were the most reproducible ($\text{COV} \leq 5\%$) against changes in all imaging settings. In addition, the IDMN feature from GLCM, LALGLE, SALGLE and LGLZE from GLSZM, and SDLGLE from GLDM feature sets were the features that were less reproducible ($\text{COV} > 20\%$) against changes in all imaging settings. Matrix size has the greatest impact on feature variability as most of features are not repeatable and 82.76% of them had ($\text{COV} > 20\%$).

Conclusion: Repeatability and reproducibility of SPECT/CT radiomics texture features in different imaging settings is feature-dependent, and different image acquisitions and reconstructions have different effects on radiomics texture features. Low COV radiomics features could be consider for further clinical studies.

Keywords: SPECT-CT, Radiomics, Cardiac, Repeatability, Reproducibility

Introduction

As major causes of death, cardiovascular diseases (CVDs) are main concerns for many scientists worldwide (1, 2). Myocardial perfusion imaging (MPI) is a valuable approach to identify CVDs patients for medical management such as diagnosis, intervention, therapy, and follow-up (3). With this regards, nuclear medicine modalities including single photon emission computed tomography (SPECT) remains the most common procedure in the evaluation and risk stratification of patients with known or suspected CVDs (4). Studies have indicated that SPECT and SPECT-CT have high diagnostic accuracy, low radiation exposure, and high image quality for CVD management (5). Advances in cardiac nuclear medicine imaging in terms of software and hardware such as optimal detector geometric arrays, linear count statistics, count rate response, and new reconstruction algorithms, provide further improvement in image quality (6, 7).

Recently, quantitative radiomics studies have opened new horizons for better medical management of several diseases such as cancer and CVDs (8-13). The aim of radiomics is to extract quantitative features from medical images using data-mining algorithms for predicting, prognosis, and therapeutic response prediction and assessment (8, 14, 15). In this light, radiomics could provide valuable information for personalized therapy. Previous radiomics studies have suggested that radiomics features could act as biomarkers that characterize and predict diseases to provide support for patient management (8, 16).

Based on biomarker discovery guidelines and studies, biomarker repeatability and reproducibility are critical and essential assessments that should be addressed prior to clinical decision making. (17). In the repeatability and reproducibility measurements, a reliable radiomic feature remains stable between two measurements when conditions remain stable. The feature should also remain the same while using different equipment, software, settings, or operator (18). If so, then the feature

may be considered as a good biomarker for clinical settings. Due to this, a considerable amount of literature has been published on radiomics features repeatability and reproducibility against changes in the radiomics process such as image acquisition, reconstruction, pre-processing, segmentation, and data analysis (19-21). Nuclear radiomics studies have tested the repeatability and reproducibility of imaging features over various imaging parameters including reconstruction algorithms, matrix size, iteration number, number of subsets, and post-filtering in both phantom and patients(18, 21).

To date, little evidence has been found on cardiac SPECT repeatability and reproducibility over different imaging settings. This present study aims to assess the repeatability and reproducibility of radiomics features for cardiac phantoms against variations in image acquisitions and reconstruction methods.

Material and Methods:

Strategy of Study

Fig 1 shows the details of the current study.

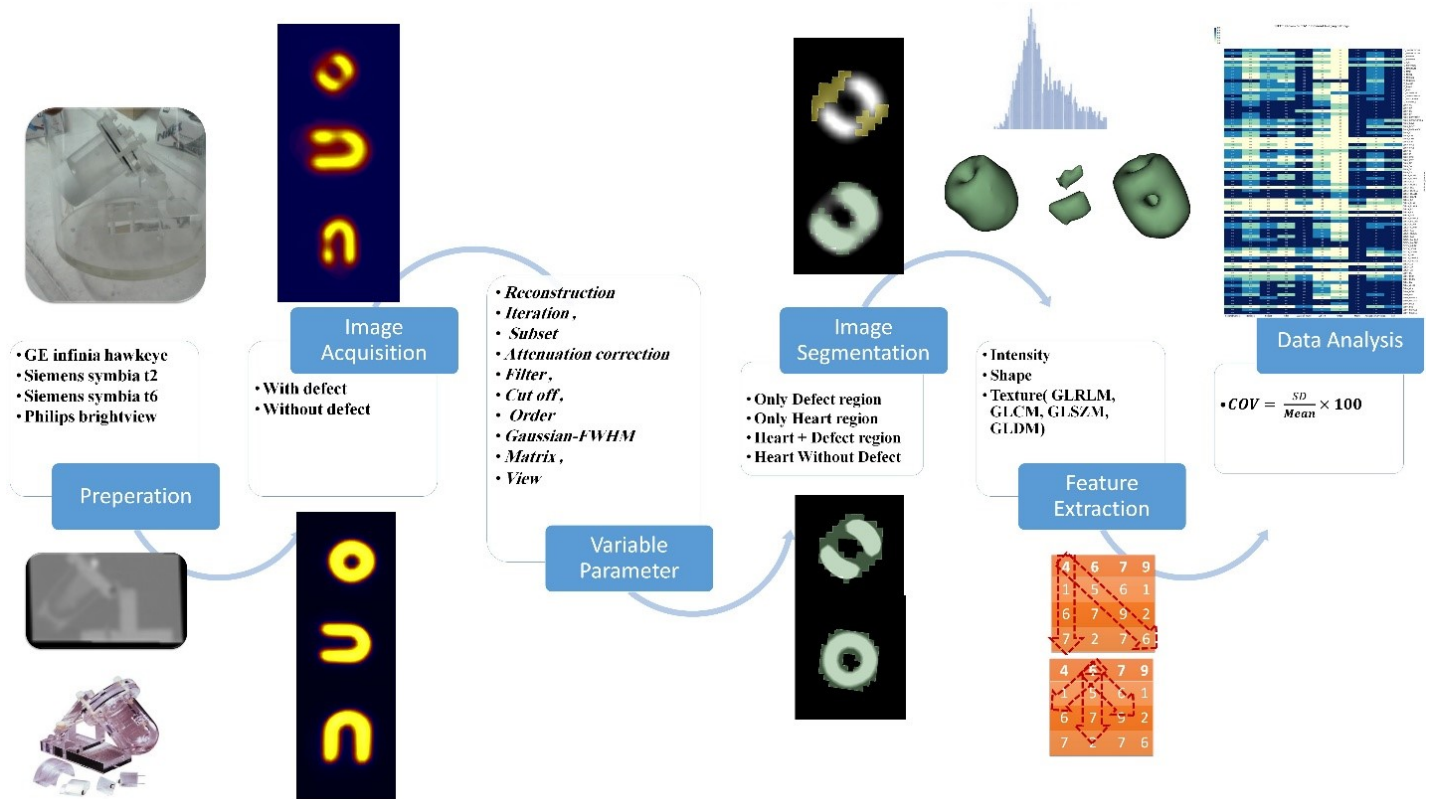


Figure 1. Illustrates the process flow followed in the paper.

Scanners

Four scanners with dual-head gamma cameras were used to acquire SPECT scans of a phantom with cardiac defects. Clinical data was obtained using three SPECT/CT scanners (GE INFINIA HAWKEYE, SIEMENS SYMBIA T2, SIEMENS SYMBIA T6, and PHILIPS BRIGHTVIEW)

Phantom Preparation

A commercially available phantom mimicking the shape of a normal heart was used in these experiments. The right ventricular cavity was filled with a solution of water, -Sestamibi (MIBI),

and only 5mCi of ^{99m}Tc to avoid any saturation-related loss in counts. This phantom was placed in the Jaszczak Phantom and was surrounded by water. In order to simulate the real position of the cardiac in the chest, the Jaszczak Phantom was placed in the center of the field of view and orientated in the 45 left-anterior and 45 caudal directions.

Data acquisition

Time per projection was modulated to obtain a total recorded activity of approximately 500 kilocounts. Three defects were also added in order to simulate clinical abnormalities. Data acquisitions were performed at different scanners with different acquisition modes such as Number of View, View Matrix Size, and attenuation correction.

Image Reconstruction

To study the impact of reconstruction settings on image features, six image reconstruction methods were used: Filter Back Projection (FBP), Ordered Subset Expectation Maximization (OSEM), Maximum Likelihood Expectation Maximization (MLEM) reconstruction, FLASH 3D, ASTONISH, and WALLIS. The effects of different settings including number of iterations, number of subsets, different filter (Butterworth, Hanning, Metz, Shepp Logan, Gaussian, Parzan), full width at half maximum (FWHM) of Gaussian filter, Butterworth filter order, and Butterworth filter cut-off were also studied. All these parameters are listed in Table 1 and resulted in 5263 reconstructed images.

Image Segmentation

All segmentations were performed using the 3D-Slicer software. For the non-defected cardiac, the whole cardiac was segmented. For the defected cardiac, three regions were extracted including the defect region, whole cardiac, and whole cardiac minus defect area. To minimize the impact of segmentation on the results, one VOI was delineated and registered on all reconstruction methods.

Table 1. The variable and constant parameters

Parameter studied	variable	stable
Reconstruction algorithm	FBP , OSEM , FLASH 3D, ASTONISH, MLEM, WALLIS	Iteration=2 , Subset=8, Filter=BW ,Cutoff=.5 , Order=10 , Matrix=64 ,View=64
Iteration	1, 2, 3, 4, 6, 8, 10, 12, 14, 16, 25	FWHM= 5mm , View=32 , Matrix=64
Subset	2, 4, 8, 16	Iteration=2 , FWHM=5mm Matrix=64 , view=32
Filter (FWHM in mm)	0, 0.5, 1, 1.5, 2, 2.5, 3, 3.5, 4, 4.5, 5, 5.5, 6, 6.5, 7	Iteration=2 , Subset=8 Matrix=64 , View=64
FILTER	Butterwort, hanning, metz, shepp logan, gussian, sheep logan, par	Matrix=64 , View=64 cutoff=.5 , Order=10
CUTOFF	.35, .4, .45, .5, .55	Matrix=64 , View=32 Filter=BW , Order=10
ORDER	1.5, 1.75, 2, 5, 9, 10, 20, 30	Matrix=64 , View=32 Filter=BW , Cut off=.5
Attenuation Correction	Device type	Matrix=64 , View=64 ,Filter=BW , cutoff=.5 , Order=10
MATRIX	64, 128, 256	View=64 , Filter=BW Cutoff=.5 , Order=5
VIEW	32, 64, 128	Matrix=64 , Filter=BW Cut off=.5 , Order=5

Feature Extraction

Eighty-seven radiomic features including first, second, and high order texture were extracted from images. Table 2 shows the extracted image features.

Statistical Analysis

To assess reproducibility and repeatability the coefficient of variation (COV) was used for each image feature over different imaging settings, by:

$$COV = \frac{SD}{Mean} \times 100$$

Where SD is the standard deviation of feature values and Mean is the mean of different settings. COVs were analyzed and four reproducibility categories were obtained based on the COV values: very small ($COV \leq 5\%$), small ($5\% < COV \leq 10\%$), intermediate ($10\% < COV \leq 20\%$) and large ($COV > 20\%$).

Results:

Figure 2 depicts the heatmap of radiomics features in different imaging settings based on COV values: 1: very small ($COV \leq 5\%$), 2: small ($5\% < COV \leq 10\%$), 3: intermediate ($10\% < COV \leq 20\%$) and 4: large ($COV > 20\%$). Table 3 provides the percentage of different COV groups in the different imaging settings.

Impact of reconstruction, number of iterations and number of subsets

For reconstruction, 16.90% (14 features) and 42.53% (37 features) of all features were found as most ($COV \leq 5\%$), and less reproducible ($COV > 20\%$), respectively. Details on these features are available in supplementary Table 1. Most of the less reproducible features were from GLRLM, GLSZM, and GLDM feature sets. The most reproducible features against reconstruction are 2 features of FO, 7 features of GLCM, 5 features of GLRLM, 2 features of GLSZM, and a feature of GLDM; as seen in supplementary Table 1. These features are 10Percentile/Entropy (from the FO feature sets), CS/ IDMN/IDN/Imc1/Imc2/JENT/SE (from the GLCM feature sets), LRE/RE/RLNUN/RP/SRE (from the GLRLM feature sets), SZE/ZP (from the GLSZM feature sets), and DE (from the GLDM feature sets).

On the impact of the number of iterations, it was found that 28.74% of all features had $COV \leq 5\%$ (25 features). Features including Entropy/Kurtosis/Mean/Median/RMS (from the FO feature sets), CS/DENT/IDMN/IDN/IMC1/IMC2/JENE/JENT/SE (from the GLCM feature sets), LRE/RE/RLNU/RLNUN/RP/SRE (from the GLRLM feature sets), SZNUN/SAE/ZE/ZP (from the GLSZM feature sets) and DE/SDE (from the GLDM feature sets) had the highest reproducibility ($COV \leq 5\%$). From the GLCM and FO feature sets, just one feature was found as less reproducible ($COV > 20\%$). These features were Minimum and CP from the FO and GLCM feature sets, respectively. More details are available in supplementary Table 2.

SPECT Radiomics COV in Different Imaging Settings

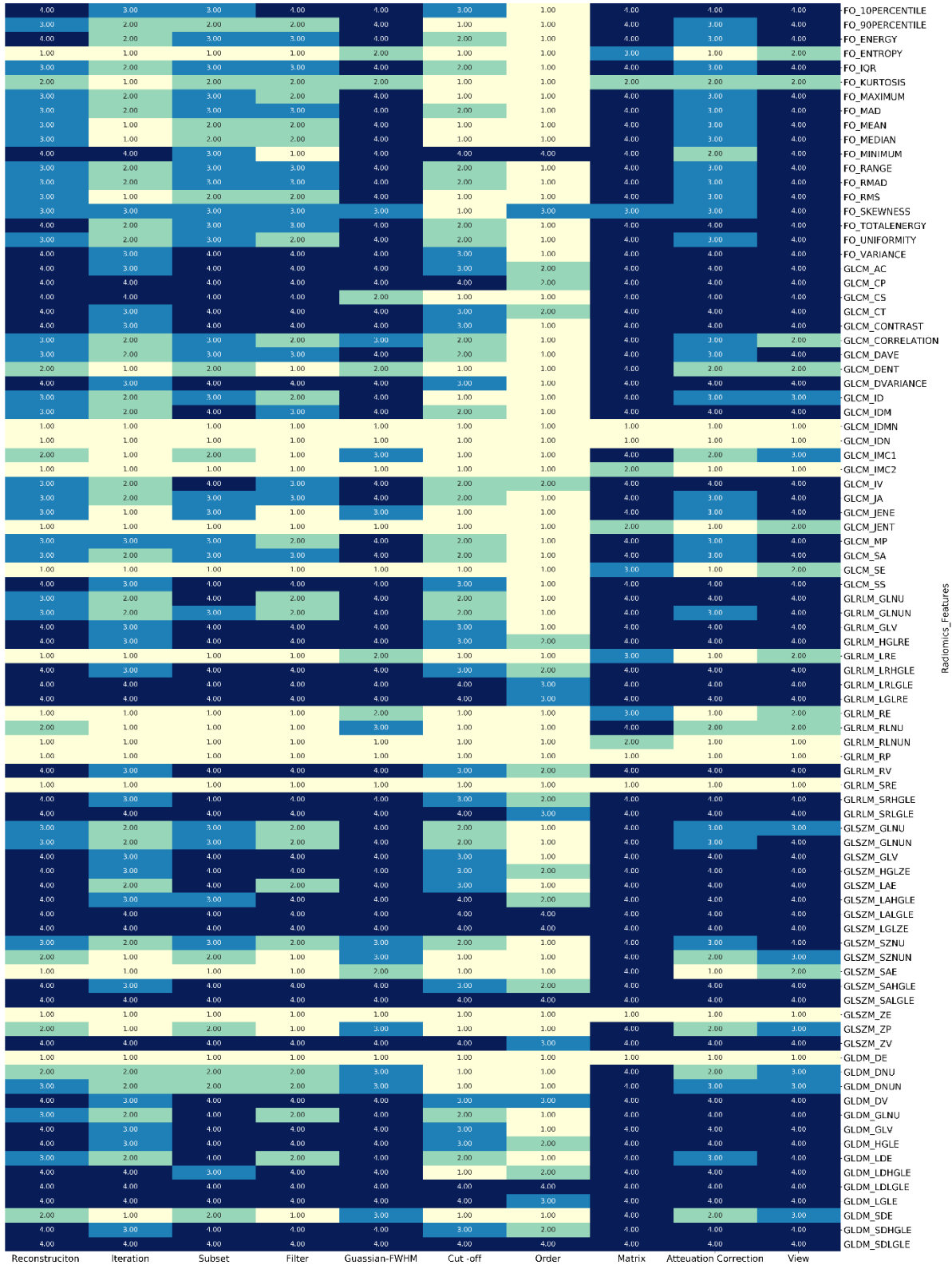
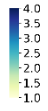


Figure 2. SPECT radiomics COV in different Imaging setting

In regards to the impact of the number of subsets on feature reproducibility, 17.24% (15 features) and 41.38% (36 features) of all features had $COV \leq 5\%$ and $COV > 20\%$ respectively. From FO feature set, Variance was the less reproducible feature ($COV > 20\%$) and from GLDM, only DE was the most reproducible feature ($COV > 20\%$). In addition, features including Entropy Minimum, CS, IDMN, IDN, IMC1, IMC2, JENT, SE, LRE, RE, RLNU, RLNUN, RP, SRE, SAE, and ZE from different feature sets had a $COV \leq 5\%$ and were introduced as the most reproducible feature. On the other hand, features AC, CP, CT, Contrast, DVARIANCE, IDM, IV, SS, GLNU, GLV, HGLRE, LRHGLE, LRLGLE, LGLRE, RV, SRHGLE, SRLGLE, GLV, HGLZE, LAE, LALGLE, LGLZE, SAHGLE, SALGLE, ZV, DV, GLNU, GLV, HGLE, LDE, LDLGLE, LGLE, SDHGLE, and SDLGLE had the highest variations against change in the number of subsets ($COV > 20\%$). More details are available in supplementary Table 3.

Impacts of Different Filter, FWHM of Gaussian filter, and Cut-off and Order of Butterworth filter

Results on the impact of filter showed that 22.59% of all features (22 FEATURES), had $COV \leq 5\%$ and features including 10percentile/Entropy/Minimum (from the FO feature set), DENT/IDMN/IDN/IMC1/IMC2/JENE/JENT/SE (from the GLCM feature set), LRE/RE/RLNU/RLNUN/RP/SRE (from the GLRLM feature set), SZNUN/SAE/ZE/ZP (from the GLSZM feature set), and DE/SDE (from the GLDM feature set) were the most reproducible features. Of the less reproducible features, 33.79% of all features (33 features) had $COV > 20\%$ and several features from GLCM, GLRLM, GLSZM, and GLDM feature sets were found as less reproducible ($COV > 20\%$). More details are available in supplementary Table 4.

On the impact of Gaussian-FWHM, results showed that 11.49% (10 features) and 67.82% (59 features) of all features had $COV \leq 5\%$ and $COV > 20\%$, respectively. Interestingly, from the FO,

GLSZM, and GLDM features sets, just one feature was found as most reproducible ($COV \leq 5\%$). These features were 10 percentile (FO), ZE (GLSZM) and DE (GLDM). On the other hand, a wide range of features was found as less reproducible ($COV > 20\%$). These features are detailed in supplementary Table 5.

Results for order showed that 37.93% (33 features) and 68.97% (60 features) of all features were most reproducible ($COV \leq 5\%$), respectively. Interestingly for GLCM and GLRLM feature sets, there was no less reproducible feature ($COV > 20\%$). For FO features, just Skewness and Minimum were not reproducible ($COV > 5\%$). In addition, for GLSZM and GLDM feature sets, features including LALGLE/LGLZE/SALGLE and LDLGLE/SDLGLE had $COV > 20\%$. More details are available in supplementary Table 6.

Regarding the cut off, results showed that 37.93% (33 features) of all features were most reproducible ($COV \leq 5\%$). For GLCM and FO feature sets, CP and Minimum were the less reproducible ($COV > 20\%$) feature, respectively. More details are available in supplementary Table 7.

Impact of Matrix size

On the impact of matrix size, data shows that most features are not repeatable and 82.76% of them had $COV > 20\%$. On the other hand, only seven features including IDMN IDN/IMC1/ (from GLCM), RP/SRE, (from GLRLE), ZE (from GLSZM), and DE (GLDM) were found as most reproducible ($COV \leq 5\%$) and there were no reproducible features from the FO feature set. More details are available in supplementary Table 8.

Impact of Attenuation Correction

The results on the impact of attenuation correction showed that 16.09% of all features (16 features) had $COV \leq 5\%$. These features are 10percentile/Entropy (from the FO feature set),

CS/IDMN/IDN/IMC1/IMC2/JENT/SE (from the GLCM feature set), LRE/RE/RLNUN/RP/SRE (from GLRLM feature set), SAE/ZE (from the GLSZM feature set), and DE (from the GLDM feature set). In addition, 44.83% (39 features) of all features were less reproducible. More details are available in supplementary Table 9.

Impact of number of views

On the impact of the number of views, results showed that 70.11% (61 features) and 9.2% (8 features) of all features had $COV \leq 5\%$ and $COV > 20\%$, respectively. Features including IDMN/IDN/IMC1/IMC2 (from the GLCM feature set), RLNUN/RP/SRE (from the GLRLM feature set), ZE (from the GLSZM feature set), and DE (from the GLDM feature set) were the most reproducible features ($COV \leq 5\%$) and there was feature with $COV \leq 5\%$ in FO feature set. More details are available in supplementary Table 10.

Table 3. The Percent of different COV group in different imaging setting

COV	Reconstruction	Iteration	Subset	Filter	Gaussian-FWHM	Cut-off	Order	Matrix	Attenuation Correction	Number of View
$COV \leq 5\%$	16.09	28.74	17.24	25.29	11.49	37.93	68.97	6.9	16.09	9.2
$5\% < COV \leq 10\%$	9.2	29.89	13.79	22.99	8.05	24.14	16.09	4.6	10.34	11.49
$10\% < COV \leq 20\%$	32.18	25.29	27.59	13.79	12.64	22.99	8.05	5.75	28.74	9.2
$COV > 20\%$	42.53	16.09	41.38	37.93	67.82	14.94	6.9	82.76	44.83	70.11

Supplemental Table 1. Effect of reconstruction

Feature category	Feature parent	COV≤5%	5%<COV≤10%	10%<COV≤20%	COV>20%
First order	FO	10Percentile/ Entropy	Kurtosis	90Percentile/ IQR/ Maximum/ MAD/ Mean/ Median/ Range/ RMAD/ RMS/ Skewness/ Uniformity	Energy/ Minimum/ TotalEnergy/ Variance
Second order	GLCM	CS/ Idmn/ Idn/ Imc1/ Imc2/ Jent/ SE	DEnt	Correlation/ Dave/ Id/ Idm/ IV/ JA/ JEnc/ MP/ SA	AC/ CP/ CT/ Contrast/ DVariance/ SS
Higher order	GLRLM	LRE/ RE/ RLNUN/ RP/ SRE	RLNU	GLNU/ GLNUN	GLV/ HGLRE/ LRHGLE/ LRLGLE/ LGLRE/ RV/ SRHGLE/ SRLGLE
	GLSZM	SZE/ ZP	SZNUN/ ZP	GLNU/ GLNUN/ SZNU	GLV/ HGLZE/ LAE/ LAHGLE/ LALGLE/ LGLZE/ SAHGLE/ SALGLE/ ZV
	GLDM	DE	DNU/ SDE	DNUN/ GLNU/ LDE	DV/ GLV/ HGLE/ LDHGLE/ LDLGLE/ LGLE/ SDHGLE/ SDLGLE

Supplemental Table 2. Effect of iteration

Feature category	Feature parent	COV \leq 5%	5%<COV \leq 10%	10%<COV \leq 20%	COV>20%
First order	FO	Entropy/ Kurtosis/ Mean/ Median/ RMS	90Percentile/ Energy/ IQR/ Maximum/ MAD/ Range/ RMAD/ TotalEnergy/ Uniformity	10Percentile Skewness Variance	Minimum
Second order	GLCM	CS/ DEnt/ Idmn/ Idn/ Imc1/ Imc2/ JEnE/ Jent/ SE	Correlation DAve Id Idm/ IV/ JA/ SA	AC CT Contrast DVariance MP SS	CP
Higher order	GLRLM	LRE/ RE/ RLNU/ RLNU/ RP/ SRE	GLNU GLNUN	GLV HGLRE LRHGLE RV SRHGLE	LRLGLE LGLRE SRLGLE
	GLSZM	SZNUN/ SAE/ ZE/ ZP	GLNU GLNUN LAE SZNU	GLV HGLZE LAHGLE SAHGLE	LALGLE LGLZE SALGLE ZV
	GLDM	DE/ SDE	DNU DNUN GLNU LDE	DV GLV HGLE SDHGLE	LDHGLE LDLGLE LGLE SDLGLE

Supplemental Table 3. Effect of subset

Feature category	Feature parent	COV≤5%	5%<COV≤10%	10%<COV≤20%	COV>20%
First order	FO	Entropy Minimum	90Percentile Kurtosis Mean Median RMS	10Percentile Energy IQR Maximum MAD Range RMAD Skewness TotalEnergy Uniformity	Variance
Second order	GLCM	CS Idmn Idn Imc1 Imc2 Jent SE	DEnt	Correlation DAve Id JA JEne MP SA	AC CP CT Contrast DVariance Idm IV SS
Higher order	GLRLM	LRE RE RLNU RLNUN RP SRE		GLNUN	GLNU GLV HGLRE LRHGLE LRLGLE LGLRE RV SRHGLE SRLGLE
	GLSZM	SAE ZE	SZNUN ZP	GLNU GLNUN LAHGLE SZNU	GLV HGLZE LAE LALGLE LGLZE SAHGLE SALGLE ZV
	GLDM	DE	DNU DNUN SDE	LDHGLE	DV GLNU GLV HGLE LDE LDLGLE LGLE SDHGLE SDLGLE

Supplemental Table 4. Effect of filter

Feature category	Feature parent	COV≤5%	5%<COV≤10%	10%<COV≤20%	COV>20%
First order	FO	10Percentile Entropy Minimum	90Percentile Kurtosis Maximum Mean Median RMS Uniformity	Energy IQR MAD Range RMAD Skewness TotalEnergy	Variance
Second order	GLCM	DEnt Idmn Idn Imc1 Imc2 JEne Jent SE	Correlation Id MP	DAve Idm IV JA SA	AC CP CS CT Contrast DVariance SS
Higher order	GLRLM	LRE RE RLNU RLNUN RP SRE	GLNU GLNUN		GLV HGLRE LRHGLE LRLGLE LGLRE RV SRHGLE SRLGLE
	GLSZM	SZNUN SAE ZE ZP	GLNU GLNUN LAE SZNU		GLV HGLZE LAHGLE LALGLE LGLZE SAHGLE SALGLE ZV
	GLDM	DE SDE	DNU DNUN GLNU LDE		DV GLV HGLE LDHGLE LDLGLE LGLE SDHGLE SDLGLE

Supplemental Table 5. Effect of Guassian-FWHM

Feature category	Feature parent	COV≤5%	5%<COV≤10%	10%<COV≤20%	COV>20%
First order	FO	10Percentile	Entropy Kurtosis	Skewness	90Percentile Energy IQR Maximum MAD Mean Median Minimum Range RMAD RMS TotalEnergy Uniformity Variance
Second order	GLCM	CS Idmn Idn Imc1 Imc2 Jent SE	DEnt	Correlation JEne	AC CP CT Contrast DAve DVariance Id Idm IV JA MP SA SS
Higher order	GLRLM	RLNUN RP SRE	LRE RE	RLNU	GLNU GLNUN GLV HGLRE LRHGLE LRLGLE LGLRE RV SRHGLE SRLGLE
	GLSZM	ZE	SAE	SZNU SZNUN ZP	GLNU GLNUN GLV HGLZE LAE LAHGLE LALGLE LGLZE SAHGLE SALGLE ZV
	GLDM	DE	DNU DNUN GLNU LDE	DNU DNUN SDE	DV GLNU GLV HGLE LDE LDHGLE LDLGLE LGLE SDHGLE SDLGLE

Supplemental Table 6. Effect of cut off

Feature category	Feature parent	COV≤5%	5%<COV≤10%	10%<COV≤20%	COV>20%
First order	FO	90Percentile Entropy Kurtosis Maximum Mean Median RMS Skewness	Energy IQR MAD Range RMAD TotalEnergy Uniformity	10Percentile Variance	Minimum
Second order	GLCM	CS DEnt Id Idmn Idn Imc1 Imc2 JEne Jent SE	Correlation DAve Idm IV JA MP SA	AC CT Contrast DVariance SS	CP
Higher order	GLRLM	LRE RE RLNU RLNUN RP SRE	GLNU GLNUN	GLV HGLRE LRHGLE RV SRHGLE	LRLGLE LGLRE SRLGLE
	GLSZM	SZNUN SAE ZE ZP	GLNU GLNUN SZNU	GLV HGLZE LAE SAHGLE	LAHGLE LALGLE LGLZE SALGLE ZV
	GLDM	DE DNU DNUN LDHGLE SDE	GLNU LDE	DV GLV HGLE SDHGLE	LDLGLE LGLE SDLGLE

Supplemental Table 7. Effect of order

Feature category	Feature parent	COV≤5%	5%<COV≤10%	10%<COV≤20%	COV>20%
First order	FO	10Percentile 90Percentile Energy Entropy IQR Kurtosis Maximum MAD Mean Median Range RMAD RMS TotalEnergy Uniformity Variance		Skewness	Minimum
Second order	GLCM	CS Contrast Correlation DAve DEnt DVariance Id Idm Idmn Idn Imc1 Imc2 JA JEne Jent MP SA SE SS	AC CP CT IV		
Higher order	GLRLM	GLNU GLNUN GLV LRE RE RLNU RLNUN RP SRE	HGLRE LRHGLE RV SRHGLE	LRLGLE LGLRE SRLGLE	
	GLSZM	GLNU GLNUN GLV LAE SZNU SZNUN SAE ZE ZP	HGLZE LAHGLE SAHGLE	ZV	LALGLE LGLZE SALGLE
	GLDM	DE DNU DNUN GLNU GLV LDE SDE	HGLE LDHGLE SDHGLE	DV LGLE	LDLGLE SDLGLE

Supplemental Table 8. Effect of matrix

Feature category	Feature parent	COV≤5%	5%<COV≤10%	10%<COV≤20%	COV>20%
First order	FO		Kurtosis	Entropy Skewness	10Percentile 90Percentile Energy/ IQR Maximum MAD/ Mean Median Minimum Range/ RMAD RMS TotalEnergy Uniformity Variance
Second order	GLCM	Idmn Idn Imc1	Imc2 Jent	SE	AC/ CP/ CS/ CT Contrast Correlation Dave/ DEnt DVariance Id/ Idm/ IV/ JA JEne/ MP/ SA/ SS
Higher order	GLRLM	RP SRE	RLNUN	LRE RE	GLNU GLNUN GLV HGLRE LRHGLE LRLGLE LGLRE RLNU RV SRHGLE SRLGLE
	GLSZM	ZE			GLNU GLNUN GLV HGLZE LAE LAHGLE LALGLE LGLZE SZNU SZNUN SAE SAHGLE SALGLE ZP ZV
	GLDM	DE			DNU DNUN DV GLNU GLV HGLE LDE LDHGLE LDLGLE LGLE SDE SDHGLE SDLGLE

Supplemental Table 9. Effect of view

Feature category	Feature parent	COV \leq 5%	5%<COV \leq 10%	10%<COV \leq 20%	COV>20%
First order	FO		Entropy Kurtosis		10Percentile 90Percentile Energy IQR Maximum MAD Mean Median Minimum Range RMAD RMS Skewness TotalEnergy Uniformity Variance
Second order	GLCM	Idmn Idn Imc1 Imc2	Correlation DEnt Jent SE	Id	AC CP CS CT Contrast DAve DVariance Idm IV JA JEn MP SA SS
Higher order	GLRLM	RLNUN RP SRE	LRE RE RLNU		GLNU GLNUN GLV HGLRE LRHGLE LRGLLE LGLRE RV SRHGLE SRLGLE
	GLSZM	ZE	SAE	GLNU SZNUN ZP	GLNUN GLV HGLZE LAE LAHGLE LALGLE LGLZE SZNU SAHGLE SALGLE ZV
	GLDM	DE		DNU DNUN SDE	DV GLNU GLV HGLE LDE LDHGLE LDLGLE LGLE SDHGLE SDLGLE

Supplemental Table 10. Effect of Attenuation Correction

Feature category	Feature parent	COV≤5%	5%<COV≤10%	10%<COV≤20%	COV>20%
First order	FO	10Percentile Entropy	Kurtosis Minimum	90Percentile Energy IQR Maximum MAD Mean Median Range RMAD RMS Skewness Uniformity	Total Energy Variance
Second order	GLCM	CS Idmn Idn Imc1 Imc2 Jent SE	DEnt	Correlation DAve Id JA JEne MP SA	AC CP CT Contrast DVariance Idm IV SS
Higher order	GLRLM	LRE RE RLNUN RP SRE	RLNU	GLNUN	GLNU GLV HGLRE LRHGLE LRLGLE LGLRE RV SRHGLE SRLGLE
	GLSZM	SAE ZE	SZNUN ZP	GLNU GLNUN SZNU	GLV HGLZE LAE LAHGLE LALGLE LGLZE SAHGLE SALGLE ZV
	GLDM	DE	DNUN SDE	DNUN LDE	DV GLNU GLV HGLE LDHGLE LDLGLE LGLE SDHGLE SDLGLE

Discussion

Radiomics is a new advanced approach for better disease management by using fast, non-invasive, easy, and cost effective methodology (10, 16). In this approach, features extracted from medical images are used for clinical applications and disease management (16, 22-26). However, it is important to note that radiomics suffers from fluctuation in the features against changing imaging settings, segmentation, and processing. Due to this, previous studies have suggested that radiomics features must be assessed in terms of repeatability, reproducibility, and robustness before applying them in clinical decision-making (27).

This study analyzed the reproducibility of cardiac SPECT radiomics features against changes in imaging settings including reconstruction, number of iterations, number of subsets, different filter, Gaussian-FWHM, cut-off, order, matrix size, attenuation correction, and number of views. Results showed that several features are reproducible while many of them are not. It was also found that the effects of different imaging settings are dependent on the type of setting and feature characteristics.

As shown in the heatmap, IDMN and IDN features from GLCM, RP from GLRLM, ZE from GLSZM, and DE from the GLDM feature sets were the only features that were most reproducible ($COV \leq 5\%$) against change in all imaging settings. In addition, the IDMN feature from GLCM, LALGLE, SALGLE, and LGLZE features from GLSZM and the SDLGLE feature from GLDM feature sets were the only features that were less reproducible ($COV > 20\%$) against changes in all imaging settings.

The results show that the matrix size has the greatest impact on feature variability, which is in concordance with previous studies. Previous study showed that the impact of matrix size changes

in PET/CT radiomic features(21). After matrix size, the number of views has the large impact on radiomics future values.

Cardiac radiomics is a new approach for better CVDs management. Several studies have been conducted in attempts to address this issue. Ashrafinia *et al.* (28, 29), applied texture and radiomics analysis to clinical myocardial perfusion SPECT imaging to predict coronary artery calcification (CAC) from CT imaging. A study by Kolossváry *et al.*(30), showed that radiomics features are superior to conventional quantitative computed tomographic metrics in identifying coronary plaques with napkin-ring signs. Neisius *et al.*(31) examined the diagnostic ability of cardiovascular magnetic resonance image radiomics features in differentiating between hypertensive heart disease (HHD) and hypertrophic cardiomyopathy (HCM). Their study showed that native T1 imaging discriminates between HHD and HCM patients and provides incremental value over global native T1 mapping.

The results can be applied in various clinical settings before any decision making and to design and discover more imaging biomarkers. A wide range of studies have been done on the repeatability and reproducibility of radiomic features. Recently, Traverso *et al.*(32) analyzed which types of radiomic features have been shown to be repeatable/reproducible in peer-reviewed studies, and to what degree of repeatability and reproducibility might be achievable. However, this review does not mention the presence of research conducted on SPECT radiomics features repeatability and reproducibility. To the best of our knowledge, this current study is the first work on this topic and it's results are beneficial for researchers and clinicians working in this field (9, 12, 33).

Although these results are significant, this study has some limitations. This study was conducted by using phantom and more clinical studies are needed to explore the impact of biological factors on the radiomics features.

Conclusion

This multi-scanner phantom study analyzed the reproducibility of Cardiac SPECT radiomics feature against changes in imaging settings including reconstruction, number of iterations, number of subsets, different filter, Gaussian-FWHM, cut-off, order, matrix size, attenuation correction, and number of views. Repeatability and reproducibility of SPECT/CT radiomics texture features in different imaging settings is feature-dependent. Additionally, different image acquisitions and reconstructions have different effects on radiomics texture features. Low COV radiomics features should be consider for further clinical studies.

Reference

1. Bauer UE, Briss PA, Goodman RA, Bowman BA. Prevention of chronic disease in the 21st century: elimination of the leading preventable causes of premature death and disability in the USA. *The Lancet*. 2014;384(9937):45-52.
2. Moradi S, Alizadehasl A, Dhooge J, Shiri I, Oveisi N, Oveisi M, et al. MFP-Unet: A Novel Deep Learning Based Approach for Left Ventricle Segmentation in Echocardiography. *arXiv preprint arXiv:190610486*. 2019.
3. Greenland P, Alpert JS, Beller GA, Benjamin EJ, Budoff MJ, Fayad ZA, et al. 2010 ACCF/AHA guideline for assessment of cardiovascular risk in asymptomatic adults: executive summary: a report of the American College of Cardiology Foundation/American Heart Association Task Force on practice guidelines developed in collaboration with the American Society of Echocardiography, American Society of Nuclear Cardiology, Society of Atherosclerosis Imaging and Prevention, Society for Cardiovascular Angiography and Interventions, Society of Cardiovascular Computed Tomography, and Society for Cardiovascular Magnetic Resonance. *Journal of the American College of Cardiology*. 2010;56(25):2182-99.
4. Rahmim A, Zaidi H. PET versus SPECT: strengths, limitations and challenges. *Nuclear medicine communications*. 2008;29(3):193-207.
5. Abdollahi H, Shiri I, Salimi Y, Sarebani M, Mehdinia R, Deevband MR, et al. Radiation dose in cardiac SPECT/CT: An estimation of SSDE and effective dose. *European journal of radiology*. 2016;85(12):2257-61.
6. Zaidi H. Quantitative SPECT: Recent developments in detector response, attenuation and scatter compensation techniques. *Physica Medica*. 1996:101-17.
7. Shahraki RH, Shiri I, Geramifar P, Akbarzadeh A, Sanaat AH, Ay MR. Resolution Recovery with Pre-Reconstruction Fourier Transforms Filtering for a High Resolution Animal SPECT System. *Frontiers in Biomedical Technologies*. 2018;5(3-4):74-80.
8. Lambin P, Leijenaar RT, Deist TM, Peerlings J, De Jong EE, Van Timmeren J, et al. Radiomics: the bridge between medical imaging and personalized medicine. *Nature Reviews Clinical Oncology*. 2017;14(12):749.
9. Kolossváry M, Kellermayer M, Merkely B, Maurovich-Horvat P. Cardiac computed tomography radiomics. *Journal of thoracic imaging*. 2018;33(1):26-34.
10. Abdollahi H, Mostafaei S, Cheraghi S, Shiri I, Mahdavi SR, Kazemnejad A. Cochlea CT radiomics predicts chemoradiotherapy induced sensorineural hearing loss in head and neck cancer patients: a machine learning and multi-variable modelling study. *Physica Medica*. 2018;45:192-7.
11. Al-Mallah MH. Radiomics in Hypertrophic Cardiomyopathy: The New Tool. *JACC: Cardiovascular Imaging*; 2019.
12. Kolossváry M, De Cecco CN, Feuchtner G, Maurovich-Horvat P. Advanced atherosclerosis imaging by CT: Radiomics, machine learning and deep learning. *Journal of cardiovascular computed tomography*. 2019.
13. Kolossváry M, Maurovich-Horvat P. Cardiac CT Radiomics. *CT of the Heart: Springer*; 2019. p. 715-24.
14. Abdollahi H, Mofid B, Shiri I, Razzaghdoust A, Saadipoor A, Mahdavi A, et al. Machine learning-based radiomic models to predict intensity-modulated radiation therapy response, Gleason score and stage in prostate cancer. *La radiologia medica*. 2019;124(6):555-67.
15. Abdollahi H, Mahdavi SR, Shiri I, Mofid B, Bakhshandeh M, Rahmani K. Magnetic resonance imaging radiomic feature analysis of radiation-induced femoral head changes in prostate cancer radiotherapy. *Journal of cancer research and therapeutics*. 2019;15(8):11.

16. Gillies RJ, Kinahan PE, Hricak H. Radiomics: images are more than pictures, they are data. *Radiology*. 2015;278(2):563-77.
17. Hatt M, Tixier F, Pierce L, Kinahan PE, Le Rest CC, Visvikis D. Characterization of PET/CT images using texture analysis: the past, the present... any future? *European journal of nuclear medicine and molecular imaging*. 2017;44(1):151-65.
18. Zwanenburg A, Leger S, Vallières M, Löck S. Image biomarker standardisation initiative. *arXiv preprint arXiv:161207003*. 2016.
19. Abdollahi H, Shiri I, Heydari M. Medical Imaging Technologists in Radiomics Era: An Alice in Wonderland Problem. *Iranian journal of public health*. 2019;48(1):184.
20. Shiri I, Abdollahi H, Shaysteh S, Mahdavi SR. Test-retest reproducibility and robustness analysis of recurrent glioblastoma MRI radiomics texture features. *Iranian Journal of Radiology*. 2017(5).
21. Shiri I, Rahmim A, Ghaffarian P, Geramifar P, Abdollahi H, Bitarafan-Rajabi A. The impact of image reconstruction settings on 18F-FDG PET radiomic features: multi-scanner phantom and patient studies. *European radiology*. 2017;27(11):4498-509.
22. Shiri I, Maleki H, Hajianfar G, Abdollahi H, Ashrafinia S, Hatt M, et al. PET/CT Radiomic Sequencer for Prediction of EGFR and KRAS Mutation Status in NSCLC Patients. *arXiv preprint arXiv:190606623*. 2019.
23. Shiri I, Maleki H, Hajianfar G, Abdollahi H, Ashrafinia S, Hatt M, et al. Next Generation Radiogenomics Sequencing for Prediction of EGFR and KRAS Mutation Status in NSCLC Patients Using Multimodal Imaging and Machine Learning Approaches. *arXiv preprint arXiv:190702121*. 2019.
24. Shiri I, Maleki H, Hajianfar G, Abdollahi H, Ashrafinia S, Oghli MG, et al., editors. PET/CT Radiomic Sequencer for Prediction of EGFR and KRAS Mutation Status in NSCLC Patients. 2018 IEEE Nuclear Science Symposium and Medical Imaging Conference Proceedings (NSS/MIC); 2018: IEEE.
25. Hajianfar G, Shiri I, Maleki H, Oveisi N, Haghparast A, Abdollahi H, et al. Non-Invasive MGMT Status Prediction in GBM Cancer Using Magnetic Resonance Images (MRI) Radiomics Features: Univariate and Multivariate Machine Learning Radiogenomics Analysis. *arXiv preprint arXiv:190703495*. 2019.
26. Hajianfar G, Shiri I, Maleki H, Oveisi N, Haghparast A, Abdollahi H, et al. Non-Invasive MGMT Status Prediction in GBM Cancer Using Magnetic Resonance Images Radiomics Features: Univariate and Multivariate Radiogenomics Analysis. *World Neurosurgery*. 2019.
27. Shiri I, Ghafarian P, Geramifar P, Leung KH-Y, Ghelichoghli M, Oveisi M, et al. Direct attenuation correction of brain PET images using only emission data via a deep convolutional encoder-decoder (Deep-DAC). *European radiology*. 2019:1-13.
28. Ashrafinia S, Dalaie P, Yan R, Ghazi P, Marcus C, Taghipour M, et al. Radiomics Analysis of Clinical Myocardial Perfusion SPECT to Predict Coronary Artery Calcification. *Journal of Nuclear Medicine*. 2018;59(supplement 1):512-.
29. Ashrafinia S, Dalaie P, Yan R, Huang P, Pomper M, Schindler T, et al. Application of Texture and Radiomics Analysis to Clinical Myocardial Perfusion SPECT Imaging. *Journal of Nuclear Medicine*. 2018;59(supplement 1):94-.
30. Kolossváry M, Karády J, Szilveszter B, Kitslaar P, Hoffmann U, Merkely B, et al. Radiomic features are superior to conventional quantitative computed tomographic metrics to identify coronary plaques with napkin-ring sign. *Circulation: Cardiovascular Imaging*. 2017;10(12):e006843.
31. Neisius U, El-Rewaidy H, Nakamori S, Rodriguez J, Manning WJ, Nezafat R. Radiomic analysis of myocardial native T1 imaging discriminates between hypertensive heart disease and hypertrophic cardiomyopathy. *JACC: Cardiovascular Imaging*. 2019.
32. Traverso A, Wee L, Dekker A, Gillies R. Repeatability and reproducibility of radiomic features: a systematic review. *International Journal of Radiation Oncology* Biology* Physics*. 2018;102(4):1143-58.
33. Kolossváry M, Szilveszter B, Karády J, Drobni ZD, Merkely B, Maurovich-Horvat P. Effect of image reconstruction algorithms on volumetric and radiomic parameters of coronary plaques. *Journal of cardiovascular computed tomography*. 2018.

